THE JOURNAL OF PHYSICAL CHEMISTRY Letters

Letter

pubs.acs.org/JPCL

Temperature-Dependent Permeability of the Ligand Shell of PbS Quantum Dots Probed by Electron Transfer to Benzoquinone

Kenneth O. Aruda, Miriam Bohlmann Kunz, Mario Tagliazucchi, and Emily A. Weiss*

Department of Chemistry, Northwestern University, 2145 Sheridan Road, Evanston, Illinois 60208-3113, United States

Supporting Information

ABSTRACT: This paper describes an increase in the yield of collisionally gated photoinduced electron transfer (electron transfer events per collision) from oleate-capped PbS quantum dots (QDs) to benzoquinone (BQ) with increasing temperature (from 0 to 50 °C), due to increased permeability of the oleate adlayer of the QDs to BQ. The same changes in intermolecular structure of the adlayer that increase its permeability to BQ also increase its permeability to the solvent, toluene, resulting in a decrease in viscous drag and an apparent increase in the diffusion coefficient of the QDs, as measured by diffusion-ordered spectroscopy (DOSY) NMR. Comparison of NMR and transient absorption spectra of QDs capped with flexible oleate with those capped with rigid methylthiolate provides evidence that the temperature dependence of the permeability of the oleate ligand shell is due to formation of transient gaps in the adlayer through conformational fluctuations of the ligands.

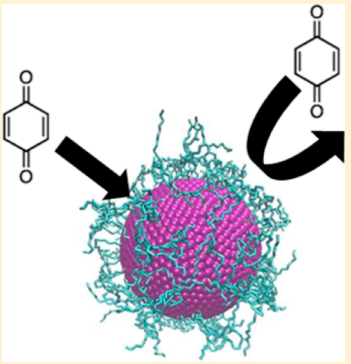

This paper describes the detection of changes in the intermolecular structure of an oleate adlayer on a PbS quantum dot (QD) as a function of temperature by monitoring the yield of collisionally gated electron transfer from the QD to benzoquinone (BQ). We observe an enhancement in the yield of collisionally gated photoinduced electron transfer with increasing temperature (from 0 to 50 °C) and show, through transient absorption and NMR studies, that this enhancement is due to increased permeability of the oleate adlayer of the QDs to BQ. The ligand shell present during the synthesis of the QDs, which is used to solubilize the QD and electronically passivate its surface, is a semipermeable self-assembled monolayer (SAM).[1] For solid state electronics, photovoltaic, or sensing applications of QDs, it makes sense to design QD films with as little organic material as possible without sacrificing passivation of the particle surfaces because the organic material is, in general, electrically insulating and increases spacing between QDs.[2,3] If, however, we are to use QDs in analytical, therapeutic, or photocatalytic applications, especially in the solution-phase, then we need to control: (1) the interaction of the QD with proximate molecules of interest while minimizing nonspecific or unproductive interactions and (2) the stability of the monolayer in various chemical environments (for example, biological environments or chemically corrosive environments).[4−6] Chemical functionalization of QDs is the most versatile, precisely tunable method for controlling their reactivity, and SAMs of organic molecules have been shown to act as molecular recognition layers for planar metal surfaces.[7−11]

The permeability of an organic adlayer on a QD can be inferred from the rate and yield of charge transfer (CT) between the QD and a redox-active probe molecule because CT between the QD and a molecule is dominated by pathways that bypass the electrically insulating layer. In the great majority of cases, CT only occurs for molecules that permeate the ligand shell and are within the tunneling radius of the QD, typically a few angstroms from the inorganic surface.[12,13] Previous studies have used cyclic voltammetry (CV) and scanning tunneling microscopy to detect heterogeneous charge transfer from conductive substrates, most frequently planar gold, to molecular probes to study intra- and intermolecular structural characteristics of the SAM, such as the conformation and tilt-angle of the molecules, the charge distribution, and the density of pinholes, "thin" regions, and adventitious adsorbates.[7−9,14−20] The relationship between the structure of an organic adlayer on a semiconductor QD and the QD's redox activity is not, however, directly analogous to (or predictable from) that relationship for a planar metal surface, as the high curvature of nanoparticle surfaces—and the presence of facets, edges, and vertices—influence the organization and density of molecules on these surfaces.[15,17,21−25] Furthermore, planar surfaces and metal NPs are amenable to CV, whereas QDs tend to undergo irreversible redox reactions and precipitate from solution under relevant applied voltages.

We instead have found that the rates of *photoinduced* CT from QDs to small molecules—both "static" CT, where the molecule is preadsorbed to the QD surface via a gap in the ligand shell, or "dynamic" CT, which occurs upon collision of the QD with a freely diffusing molecule—are sensitive probes of the static and dynamic structure of the ligand shell.[12,13,26,27] Here, we determine that, for the PbS QD-BQ system, the yield of static CT remains unchanged with varying temperature

Received: June 12, 2015
Accepted: July 6, 2015

DOI: 10.1021/acs.jpclett.5b01256
J. Phys. Chem. Lett. 2015, 6, 2841−2846

between 0 and 50 °C, but the yield of dynamic, collisionally gated CT (CT events per collision) increases with increasing temperature. The combination of transient absorption and NMR studies suggests that the temperature dependence of the collisional quenching efficiency is attributable to the temperature-sensitive dynamics of the conformationally flexible ligand shell, and that it is the fluctuations of these ligands that control the redox activity of the QD on the diffusion-limited (i.e., microsecond) time scale.

We synthesize oleate-coated PbS QDs with a band-edge absorption peak at 990 nm using a procedure modified from that of Hines and Scholes.[28] This procedure, and the procedure for purifying the QDs, are detailed in the Supporting Information. Figure 1A, black, shows the transient absorption (TA) spectrum of a solution of 1 μM PbS QDs in toluene at 0.1 μs after photoexcitation using a 950 nm pump. The negative feature centered at 990 nm is the bleach of the ground-state band-edge absorption of the QDs (GS bleach). The GS bleach recovers with the removal of either an electron or hole (or both) from the $1S_e-1S_h$ excitonic state of the QDs; depopulation of this state can occur by trapping of an excitonic carrier on the QD surface, radiative recombination, or charge transfer to a proximate redox partner.[12,13,26,29] Figure 1A, red, shows the TA spectrum of a room-temperature mixture of 1 μM PbS QDs with 10 μM of BQ in toluene at the same delay −0.1 μs after photoexcitation. The amplitude of the GS bleach is approximately half that of the PbS QDs without added BQ at the same delay time. We have shown previously[12,13] that this accelerated excited state decay is due to photoinduced electron transfer (PET) from the conduction band-edge of the PbS QD to the LUMO of BQ; the PET process has a driving force of approximately −0.3 eV.[13]

Figure 1B shows kinetic traces on the nanosecond-to-microsecond time scale, extracted at 1000 nm from the TA spectrum in Figure 1A, for a 1 μM sample of PbS QDs (black traces) and for a 1 μM sample of PbS QDs with 10 μM of added BQ (colored traces) at temperatures between 0 to 50 °C. The Supporting Information (Figures S3 and S4) contains the fits of each trace in this figure to a single exponential decay. For PbS QDs without added BQ, the excitonic state of the QDs decays exponentially with a single time constant of $\tau_{\mu s,0}$ = 2.42 ± 0.13 μs (where the uncertainty is the standard deviation of three TA measurements on three separately prepared samples), and there is no trend in this time constant with temperature. The excited state lifetimes in samples with BQ, $\tau_{\mu s}$, are accelerated to due to PET, and get shorter with increasing temperature, from 1.21 ± 0.06 μs at 10 °C to 0.78 ± 0.04 μs at 50 °C. We have established previously[12,30,31] that single-exponential kinetics of exciton decay on the microsecond time scale for the PbS QD-BQ system are indicative of diffusion-limited PET from the QD to BQ, and that the corresponding time constants are related to the bimolecular quenching constant k_q through the Stern−Volmer eq 1 for dynamic quenching of a photoexcited fluorophore.[30]

$$\frac{\tau_{\mu s,0}}{\tau_{\mu s}} = 1 + k_q \tau_{\mu s,0}[\mathrm{BQ}] \quad (1)$$

Table 1 lists the values of k_q for the QD-BQ system; these values increase with increasing temperature.

The increase in the bimolecular quenching constant, k_q, with increasing temperature is potentially due to two factors: (i) an increased frequency of collisions between the QDs and BQ or

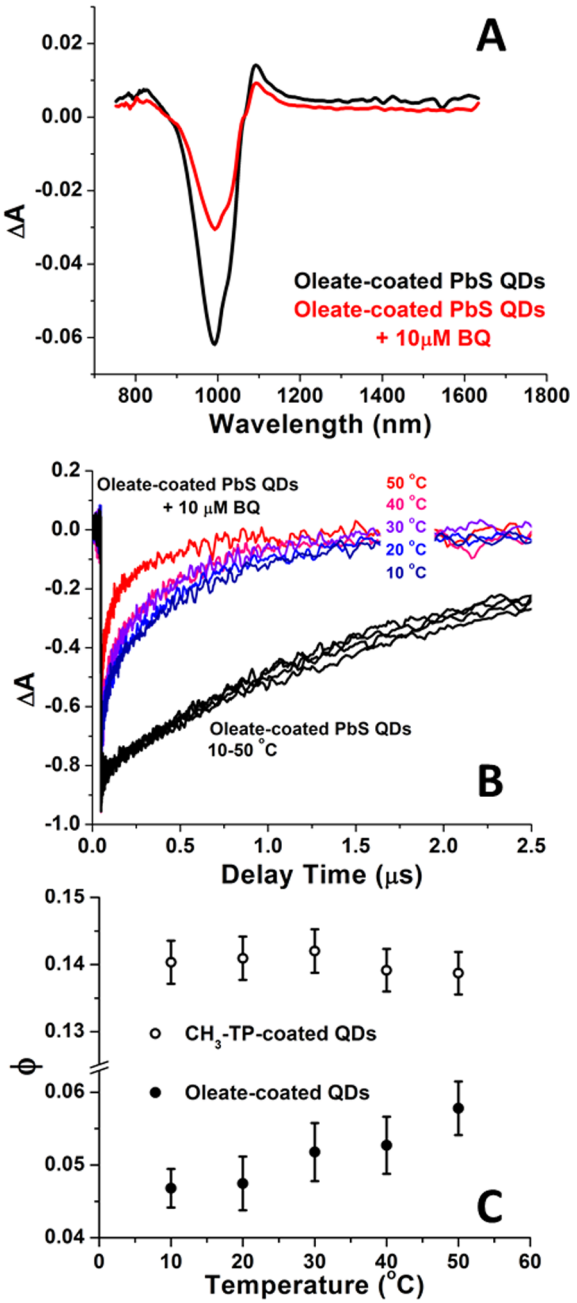

Figure 1. (A) The TA spectrum of 1 μM PbS QDs (black) and 1 μM PbS QDs with 10 μM of BQ (red) at 0.1 μs after excitation at 950 nm. The negative signal at 1000 nm is the bleach of the first excitonic transition of the QDs. The sharp positive feature at ∼1110 nm is trans-bandgap absorption of probe light by QDs that have already been excited by the pump. It is shifted from the bleach of the band-edge exciton by the exciton−exciton binding energy. (B) Kinetic traces extracted at 1000 nm from the TA spectrum in (A) of PbS QDs (black) and PbS QDs with 10 μM of BQ (colored) from 10 to 50 °C. The rate of diffusion-controlled quenching of the PbS QDs by BQ increases with increasing temperature, while the exciton recombination dynamics of the QDs without added BQ do not trend with temperature, see Table 1. (C) The yield of collisional electron transfer, Φ, calculated as described in the text, increases as temperature increases for oleate-coated PbS QDs, but is constant with temperature for CH_3-TP-coated QDs. The error bars are the uncertainties propagated from the uncertainties in both k_o and k_q, and include three separate TA measurements on separately prepared samples.

DOI: 10.1021/acs.jpclett.5b01256
J. Phys. Chem. Lett. 2015, 6, 2841−2846

Table 1. Bimolecular Quenching Constant, k_q, for the PbS QD-BQ System, as a Function of Temperature

temperature (°C)	k_q (M^{-1} s^{-1})[a]
10	$(2.61 \pm 0.14) \times 10^9$
20	$(2.78 \pm 0.15) \times 10^9$
30	$(3.58 \pm 0.17) \times 10^9$
40	$(4.35 \pm 0.21) \times 10^9$
50	$(5.03 \pm 0.22) \times 10^9$

[a]Measured by transient absorption spectroscopy. Error bars are the standard deviations propagated from the uncertainties in $\tau_{\mu s,0}$ and $\tau_{\mu s}$, as determined from TA measurements on three separately prepared samples.

(ii) an increased fraction of these collisions that result in electron transfer. In order to determine the contribution of each factor, we first use diffusion ordered spectroscopy (DOSY) NMR[26,32] to measure the diffusion coefficients for PbS QDs (D_{QD}) and BQ (D_{BQ}) at temperatures from 0 to 50 °C. Both diffusion constants are expected to vary with temperature according to the Stokes−Einstein equation, eq 2[33]

$$D = \frac{k_B T}{6\pi\eta(T)R_H} \quad (2)$$

In eq 2, k_B is the Boltzmann constant, $\eta(T)$ is the temperature-dependent viscosity of the solvent, and R_H is the hydrodynamic radius of the diffusing particle. The Supporting Information describes the procedure for DOSY NMR. Measurement of D_{BQ} is straightforward. As has been done previously by us[26,31] and others,[34] we measure D_{QD} by measuring the diffusion coefficient of oleate molecules bound to the surface of the QDs. The inset to Figure 2 shows the ^{1}H NMR spectra of a sample of 10 μM oleate-capped PbS QDs in toluene-d_8. The signals from the vinyl protons appear as a broad peak between 5.6 and 5.7 ppm for bound oleate, and as a sharp multiplet at 5.4 ppm for free oleic acid (this multiplet is not present in the spectra in Figure 2). The multiplet at ∼5.80−5.85 ppm corresponds to octadecene, another surfactant in the reaction mixture that does not displace oleate. We monitor the peak corresponding to bound oleate in the DOSY experiment to measure diffusion coefficients for the QDs that range from 0.84×10^{-10} cm^{-1} s^{-1} at 0 °C to 2.11×10^{-10} cm^{-1} s^{-1} at 50 °C. If we consider for a moment the oleate-coated QDs to be hard spheres, the corresponding hydrodynamic radii, R_H, of the particles range from 3.5 to 2.5 nm (Figure 2 and Table 2), where we have included in this calculation the known temperature dependence of the viscosity of toluene according to eq 2.[35] The Supporting Information (Figure S1) shows that we obtain the same diffusion constants for the QDs if we use peaks corresponding to the methylene or methyl protons of oleate, rather than the vinyl protons.

We then use the measured values of D_{QD} and D_{BQ} to calculate the bimolecular collision frequency (k_o) between the QDs and BQ using eq 3

$$k_o = \frac{4N_A}{1000} R_{coll}(D_{QD} + D_{BQ}) \quad (3)$$

In eq 3, N_A is Avogadro's number and R_{coll} is the collision radius, which is the sum of the hydrodynamic radii of the QD and BQ. Table 2 lists the values of k_o for the mixture of QDs and 10 μM BQ at each temperature. As expected, k_o increases with temperature.

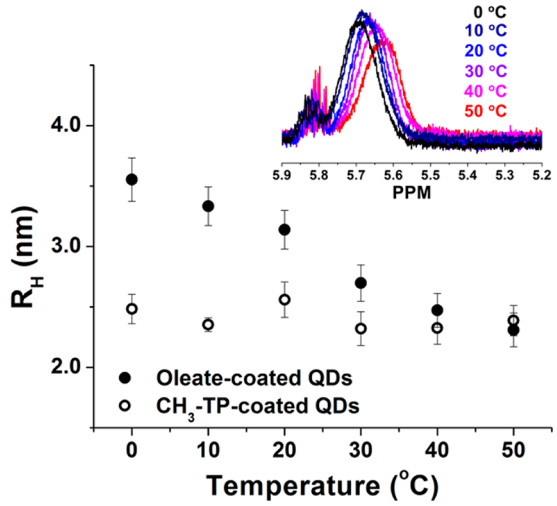

Figure 2. Hydrodynamic radii, R_H, of oleate-coated (solid) or CH_3-TP-coated (open) 10 μM PbS QDs in toluene, calculated from the diffusion coefficients of the QDs measured by DOSY NMR, as a function of temperature. The spectra for each temperature were acquired nonsequentially and any changes in the diffusion coefficients with temperature are reversible upon returning to room temperature. The error bars are the uncertainties propagated from the standard error from single exponential fits to the decay of the ^{1}H signal with magnetic field gradient and from the uncertainty in the measured solvent viscosity. *Inset*: Vinyl region of the ^{1}H NMR spectra of oleate-capped 10 μM PbS QDs at temperatures between 10 and 50 °C. The broad signal at 5.6−5.7 ppm corresponds to bound oleate and is the signal we monitor in DOSY NMR. This peak shifts with temperature; however, the magnitude of this shift is the same as that for free oleic acid in a separate experiment (see the Supporting Information, Figure S5). The signal from free oleic acid at 5.4 ppm is absent. The multiplet centered at ∼5.85 ppm corresponds to residual octadecene, which is a surfactant in the synthesis of the QDs.

Using these values of k_o, and the values of k_q determined from the dynamics of electron transfer (Figure 1B) via eq 1, we calculate the collisional quenching efficiency (the fraction of collisions that result in PET), $\Phi = k_q/k_o$, for the sample at each temperature.[12,13,26,30] Figure 1C is a plot of Φ as a function of temperature; this plot indicates that Φ, and not just the collision frequency, increases with temperature. The variation of Φ with temperature is small but statistically significant; the error bars include error propagated from both k_o and k_q. The small absolute value of Φ for all samples (ca. 5%) is consistent with previous measurements on this system.[13] It suggests that BQ must be in close proximity of the inorganic core of the QD in order to accept an electron during the lifetime of the QD's excited state and that, in general, the oleate ligand shell provides an effective barrier to transport of BQ to the QD surface. The permeation of BQ through the ligand shell limits the yield of PET, so the data in Figure 1C show that increasing the temperature increases the permeability of the oleate layer to BQ.

We now return to the result that the diffusion constant of the QDs, D_{QD}, increases as the temperature of the sample increases and thus yields a set of hydrodynamic radii for the particles that range from 3.5 nm at 0 °C to 2.5 nm at 50 °C (Figure 2 and Table 2). The radius of the QD core is 1.7 nm, and the length of a fully extended oleate ligand is 2.0 nm,[36] so the largest measured value of R_H is close to but smaller than the maximum value (3.7 nm). The decrease in the apparent radius of the oleate-capped QD with increasing temperature indicates that

DOI: 10.1021/acs.jpclett.5b01256
J. Phys. Chem. Lett. 2015, 6, 2841−2846

Table 2. Diffusion Coefficients and Apparent Hydrodynamic Radii, R_H, of PbS QDs and BQ in Toluene at 0 °C − 50 °C, and the Values of k_o for the PbS QD/BQ System

	benzoquinone		oleate-coated PbS QDs		
temperature (°C)	diffusion coefficient ($\times 10^{-4}$ cm^{-2} s^{-1})[a]	R_H (Å)[b]	diffusion coefficient ($\times 10^{-6}$ cm^{-2} s^{-1})[a]	R_H (nm)[b]	k_o ($\times 10^4$ μs^{-1})[c]
0	1.32 ± 0.06	1.95 ± 0.10	0.65 ± 0.03	3.55 ± 0.18	4.04 ± 0.17
10	1.66 ± 0.07	1.86 ± 0.09	0.82 ± 0.04	3.33 ± 0.16	5.05 ± 0.09
20	1.92 ± 0.09	1.90 ± 0.10	1.23 ± 0.06	3.13 ± 0.16	5.87 ± 0.33
30	2.26 ± 0.11	1.90 ± 0.10	1.44 ± 0.07	2.69 ± 0.15	6.92 ± 0.42
40	2.69 ± 0.14	1.85 ± 0.11	2.02 ± 0.11	2.47 ± 0.14	8.25 ± 0.47
50	2.81 ± 0.15	2.04 ± 0.12	2.62 ± 0.14	2.31 ± 0.14	8.69 ± 0.41

[a]Measured by DOSY NMR. Error bars are the standard error of single exponential fits to the decay of the ^{1}H signal with magnetic field gradient. [b]Calculated using eq 2. Error bars are the uncertainties propagated from the error in the diffusion coefficients and solvent viscosities. [c]Calculated using eq 3. Error bars are the uncertainties propagated from the error in the diffusion coefficients.

the viscous drag of the QDs decreases with increasing temperature. One interpretation of this result is that, with increasing temperature, the oleate adlayer becomes more solvent-like—that is, comprises a higher volume fraction of toluene due to changes in the intermolecular structure of the adlayer. The observation that the ligand shell is more permeable to toluene at higher temperatures is consistent with our observation, from the trend in collisional quenching efficiencies (Figure 1C), and that the ligand shell is also more permeable to BQ, which is a similar size and structure to toluene, at higher temperatures.

When we perform a near-complete (80%, see the Supporting Information, Figure S6) ligand exchange of the oleate with the short, rigid methylthiolate ligand, neither the diffusion constant of the QDs (Figure 2) nor the collisional quenching efficiency of the QD-BQ system (Figure 1C) are temperature dependent over the studied range. This result suggests that the temperature dependence of the intermolecular structure of the ligand layer, and therefore the temperature dependence of R_H and Φ, is related to the conformational motion of the flexible oleate ligands.

We do not believe that the temperature dependencies of R_H and Φ are related to a change in the density of ligands on the surface of the QD with temperature for three reasons: (i) The QDs are washed with solvents (MeOH and acetone) in which oleic acid, but not the QDs, are soluble. As shown in the NMR spectrum in the inset to Figure 2, this procedure effectively removes excess oleic acid from the sample. In aprotic solvent, desorption of oleate depends on its protonation by free oleic acid in the sample,[22,24,25] so the rate of desorption of oleate should be negligible in these samples even at elevated temperatures. (ii) The observed hydrodynamic radius, R_H, of a particle can be approximated as its core radius plus the average thickness of its ligand shell. Given the fact that (1) R_H of the oleate-coated QDs at 50 °C is within experimental uncertainty of R_H of the CH_3-TP-coated QDs (at any temperature) (see Figure 2), (2) CH_3-TP is approximately half the molecular length of oleate, and (3) CH_3-TP displaces 80% of the oleate molecules on the surface of the QD during our ligand exchange, we calculate that 40% of the oleate molecules would have to desorb from the QD in order to measure a value for R_H of 2.3 nm if desorption were the sole mechanism for the temperature dependence of R_H. This total concentration of oleate (~400 μM) is certainly detectable by NMR, but we do not see it at any temperature in Figure 2, inset. (iii) We have shown previously[27,37] that the ligand density on the surface of the QD is inversely correlated with the number of small molecules (like BQ) that adsorb to the QD upon equilibration of the QD-BQ mixture. These adsorbed small molecules, if redox-active, typically participate in ultrafast (picosecond-time scale) electron transfer rather than the diffusion-limited electron transfer with the QD that we monitor in Figure 1B. The observed rate constant for ultrafast electron transfer scales approximately linearly with the number of adsorbed electron acceptors,[38,39] so if the density of protective oleate ligands on the surface of the QD were decreasing with increasing temperature, the rate constant for ultrafast electron transfer would increase with increasing temperature. In contrast, the picosecond-time scale dynamics of the GS bleach are independent of temperature (see the Supporting Information, Figure S2).

In summary, we have established that increasing the temperature of PbS QD-BQ mixtures increases the probability that BQ will accept an electron from a photoexcited QD upon colliding with it by increasing the permeability of the organic adlayer on the QDs to BQ. We have observed that the diffusion-controlled electron transfer rate for this system is sensitive to small changes in the intermolecular structure of the QD's ligands. The increase in collisional quenching efficiency of the QD-BQ system with increasing temperature is correlated with a decrease in the apparent hydrodynamic radius of the QD, measured by DOSY NMR, which we attribute to an increase in the permeability of the ligand shell to the solvent, toluene, and a resultant decrease in the viscous drag of the QD. The temperature dependence of both the apparent hydrodynamic radius of the QDs and the collisional quenching efficiency disappear upon replacement of oleate with conformationally inflexible methylthiophenolate.

The absence of a mechanism for oleate desorption, the insensitivity of the picosecond-time scale PET dynamics of the system to temperature, and the absence of any signal from desorbed oleate in the NMR suggest that the temperature dependence of the permeability of the adlayer is not related to a change in ligand density, but rather to the temperature dependence of the dynamic fluctuations of the flexible ligand shell. These fluctuations gate the permeation of small molecules (like BQ and toluene) through the ligand shell to the surface of the QD by creating transient defects (gaps). The yield of photoinduced electron transfer is a sensitive probe of these fluctuations if these transient gaps are of a similar size to the small molecule redox probe. If the solvent molecules are also the size of these gaps, then DOSY NMR, a very slow-time scale experiment, is also a useful measurement of ligand fluctuations within organic adlayers on small colloids. This work suggests that in designing QD-based heterogeneous or homogeneous photocatalytic systems, where catalysis occurs through

DOI: 10.1021/acs.jpclett.5b01256
J. Phys. Chem. Lett. 2015, 6, 2841−2846

diffusion-controlled redox processes, one should consider not only the degree of chemical and electronic passivation provided by the headgroup of the ligand but also the average density and local dynamic behavior of molecules within the ligand shell.

■ ASSOCIATED CONTENT

Supporting Information

Additional experimental details; details of synthesis and characterization of PbS QDs, setup for the transient absorption experiments; picosecond and microsecond transient absorption kinetics and temperature dependent ^{1}H NMR spectra of free and bound oleic acid. The Supporting Information is available free of charge on the ACS Publications website at DOI: 10.1021/acs.jpclett.5b01256.

■ AUTHOR INFORMATION

Corresponding Author

*Email: e-weiss@northwestern.edu.

Notes

The authors declare no competing financial interest.

■ ACKNOWLEDGMENTS

This material is based upon work supported by the National Science Foundation under CHE-1400596.

■ REFERENCES

(1) Love, J. C.; Estroff, L. A.; Kriebel, J. K.; Nuzzo, R. G.; Whitesides, G. M. Self-Assembled Monolayers of Thiolates on Metals as a Form of Nanotechnology. *Chem. Rev. (Washington, DC, U. S.)* **2005**, *105*, 1103−1170.

(2) Tang, J.; et al. Colloidal-Quantum-Dot Photovoltaics Using Atomic-Ligand Passivation. *Nat. Mater.* **2011**, *10*, 765−771.

(3) Liu, W.; Lee, J.-S.; Talapin, D. V. III−V Nanocrystals Capped with Molecular Metal Chalcogenide Ligands: High Electron Mobility and Ambipolar Photoresponse. *J. Am. Chem. Soc.* **2012**, *135*, 1349−1357.

(4) Brown, K. A.; Dayal, S.; Ai, X.; Rumbles, G.; King, P. W. Controlled Assembly of Hydrogenase-CdTe Nanocrystal Hybrids for Solar Hydrogen Production. *J. Am. Chem. Soc.* **2010**, *132*, 9672−9680.

(5) Hines, D. A.; Kamat, P. V. Quantum Dot Surface Chemistry: Ligand Effects and Electron Transfer Reactions. *J. Phys. Chem. C* **2013**, *117*, 14418−14426.

(6) Pagba, C.; Zordan, G.; Galoppini, E.; Piatnitski, E. L.; Hore, S.; Deshayes, K.; Piotrowiak, P. Hybrid Photoactive Assemblies: Electron Injection from Host−Guest Complexes into Semiconductor Nanoparticles. *J. Am. Chem. Soc.* **2004**, *126*, 9888−9889.

(7) Chailapakul, O.; Crooks, R. M. Interactions between Organized, Surface-Confined Monolayers and Liquid-Phase Probe Molecules 0.4. Synthesis and Characterization of Nanoporous Molecular Assemblies - Mechanism of Probe Penetration. *Langmuir* **1995**, *11*, 1329−1340.

(8) Zhang, H. L.; Chen, M.; Li, H. L. Study on Two-Component Matrix Formed by Coadsorption of Aromatic and Long Chain Mercaptans on Gold. *J. Phys. Chem. B* **2000**, *104*, 28−36.

(9) Ullman, A. Formation and Structure of Self-Assembled Monolayers. *Chem. Rev. (Washington, DC, U. S.)* **1996**, *96*, 1533−1554.

(10) Ito, T.; et al. Self-Assembled Monolayers of Alkylphosphonic Acid on GaN Substrates. *Langmuir* **2008**, *24*, 6630−6635.

(11) Meulenberg, R. W.; Bryan, S.; Yun, C. S.; Strouse, G. F. Effects of Alkylamine Chain Length on the Thermal Behavior of CdSe Quantum Dot Glassy Films. *J. Phys. Chem. B* **2002**, *106*, 7774−7780.

(12) Knowles, K. E.; Tagliazucchi, M.; Malicki, M.; Swenson, N. K.; Weiss, E. A. Electron Transfer as a Probe of the Permeability of Organic Monolayers on the Surfaces of Colloidal PbS Quantum Dots. *J. Phys. Chem. C* **2013**, *117*, 15849−15857.

(13) Knowles, K. E.; Malicki, M.; Weiss, E. A. Dual-Time Scale Photoinduced Electron Transfer from PbS Quantum Dots to a Molecular Acceptor. *J. Am. Chem. Soc.* **2012**, *134*, 12470−12473.

(14) Donakowski, M. D.; Godbe, J. M.; Sknepnek, R.; Knowles, K. E.; de la Cruz, M. O.; Weiss, E. A. A Quantitative Description of the Binding Equilibria of *para*-Substituted Aniline Ligands and CdSe Quantum Dots. *J. Phys. Chem. C* **2010**, *114*, 22526−22534.

(15) Bandyopadhyay, K.; Patil, V.; Sastry, M.; Vijayamohanan, K. Effect of Geometric Constraints on the Self-Assembled Monolayer Formation of Aromatic Disulfides on Polycrystalline Gold. *Langmuir* **1998**, *14*, 3808−3814.

(16) Dolidze, T. D.; Rondinini, S.; Vertova, A.; Longhi, M.; Khoshtariya, D. E. Charge-Transfer Patterns for $[Ru(NH_3)_6]^{3+/2+}$ at SAM Modified Gold Electrodes: Impact of the Permeability of a Redox Probe. *Open Phys. Chem. J.* **2008**, *2*, 17−21.

(17) Lee, T.; Wang, W.; Klemic, J. F.; Zhang, J. J.; Su, J.; Reed, M. A. Comparison of Electronic Transport Characterization Methods for Alkanethiol Self-Assembled Monolayers. *J. Phys. Chem. B* **2004**, *108*, 8742−8750.

(18) Salomon, A.; Cahen, D.; Lindsay, S.; Tomfohr, J.; Engelkes, V. B.; Frisbie, C. D. Comparison of Electronic Transport Measurements on Organic Molecules. *Adv. Mater. (Weinheim, Ger.)* **2003**, *15*, 1881−1890.

(19) Slowinski, K.; Chamberlain, R. V.; Miller, C. J.; Majda, M. Through-Bond and Chain-to-Chain Coupling. Two Pathways in Electron Tunneling through Liquid Alkanethiol Monolayers on Mercury Electrodes. *J. Am. Chem. Soc.* **1997**, *119*, 11910−11919.

(20) Tran, E.; Rampi, M. A.; Whitesides, G. M. Electron Transfer in a Hg-SAM//SAM-Hg Junction Mediated by Redox Centers. *Angew. Chem.* **2004**, *116*, 3923−3927.

(21) Badia, A.; Lennox, R. B.; Reven, L. A Dynamic View of Self-Assembled Monolayers. *Acc. Chem. Res.* **2000**, *33*, 475−481.

(22) Ganesh, V.; Lakshminarayanan, V. Self-Assembled Monolayers of Alkanethiols on Gold Prepared in a Hexagonal Lyotropic Liquid Crystalline Phase of Triton X-100/Water System. *Langmuir* **2006**, *22*, 1561−1570.

(23) Subramanian, S.; Sampath, S. Enhanced Stability of Short- and Long-Chain Diselenide Self-Assembled Monolayers on Gold Probed by Electrochemistry, Spectroscopy, and Microscopy. *J. Colloid Interface Sci.* **2007**, *312*, 413−424.

(24) Templeton, A. C.; Wuelfing, M. P.; Murray, R. W. Monolayer Protected Cluster Molecules. *Acc. Chem. Res.* **2000**, *33*, 27−36.

(25) Weeraman, C.; Yatawara, A. K.; Bordenyuk, A. N.; Benderskii, A. V. Effect of Nanoscale Geometry on Molecular Conformation: Vibrational Sum-Frequency Generation of Alkanethiols on Gold Nanoparticles. *J. Am. Chem. Soc.* **2006**, *128*, 14244−14245.

(26) Malicki, M.; Knowles, K. E.; Weiss, E. A. Gating of Hole Transfer from Photoexcited PbS Quantum Dots to Aminoferrocene by the Ligand Shell of the Dots. *Chem. Commun. (Cambridge, U. K.)* **2013**, *49*, 4400−4402.

(27) Morris-Cohen, A. J.; Vasilenko, V.; Amin, V. A.; Reuter, M. G.; Weiss, E. A. Model for Adsorption of Ligands to Colloidal Quantum Dots with Concentration-Dependent Surface Structure. *ACS Nano* **2012**, *6*, 557−565.

(28) Hines, M. A.; Scholes, G. D. Colloidal PbS Nanocrystals with Size-Tunable near-Infrared Emission: Observation of Post-Synthesis Self-Narrowing of the Particle Size Distribution. *Adv. Mater. (Weinheim, Ger.)* **2003**, *15*, 1844−1849.

(29) Knowles, K. E.; Malicki, M.; Parameswaran, R.; Cass, L. C.; Weiss, E. A. Spontaneous Multi-Electron Transfer from the Surfaces of PbS Quantum Dots to TCNQ. *J. Am. Chem. Soc.* **2013**, *135*, 7264−7271.

(30) Knowles, K. E.; Peterson, M. D.; McPhail, M. R.; Weiss, E. A. Exciton Dissociation within Quantum Dot-Organic Complexes: Mechanisms, Use as a Probe of Interfacial Structure, and Applications. *J. Phys. Chem. C* **2013**, *117*, 10229−10243.

(31) Knowles, K. E.; Tice, D. B.; McArthur, E. A.; Solomon, G. C.; Weiss, E. A. Chemical Control of the Photoluminescence of Cdse

DOI: 10.1021/acs.jpclett.5b01256
J. Phys. Chem. Lett. 2015, 6, 2841−2846

Quantum Dot-Organic Complexes with a Series of *para*-Substituted Aniline Ligands. *J. Am. Chem. Soc.* **2010**, *132*, 1041−1050.
(32) Fritzinger, B.; Martins, J. C.; Moreels, I.; Lommens, P.; Koole, R.; Hens, Z. In Situ Observation of Rapid Ligand Exchange in Colloidal Nanocrystal Suspensions Using Transfer NOE Nuclear Magnetic Resonance Spectroscopy. *J. Am. Chem. Soc.* **2009**, *131*, 3024−3032.
(33) Edward, J. T. Molecular Volumes and the Stokes-Einstein Equation. *J. Chem. Educ.* **1970**, *47*, 261.
(34) Hens, Z.; Martins, J. C. A Solution NMR Toolbox for Characterizing the Surface Chemistry of Colloidal Nanocrystals. *Chem. Mater.* **2013**, *25*, 1211−1221.
(35) Harris, K. R. Temperature and Density Dependence of the Viscosity of Toluene. *J. Chem. Eng. Data* **2000**, *45*, 893−897.
(36) Cass, L. C.; Malicki, M.; Weiss, E. A. The Chemical Environments of Oleate Species within Samples of Oleate-Coated PbS Quantum Dots. *Anal. Chem.* **2013**, *85*, 6974−6979.
(37) Morris-Cohen, A. J.; Frederick, M. T.; Cass, L. C.; Weiss, E. A. Simultaneous Determination of the Adsorption Constant and the Photoinduced Electron Transfer Rate for a CdS Quantum Dot-Viologen Complex. *J. Am. Chem. Soc.* **2011**, *133*, 10146−10154.
(38) Boulesbaa, A.; Issac, A.; Stockwell, D.; Huang, Z.; Huang, J.; Guo, J.; Lian, T. Ultrafast Charge Separation at CdS Quantum Dot/Rhodamine B Molecule Interface. *J. Am. Chem. Soc.* **2007**, *129*, 15132−15133.
(39) Song, N.; Zhu, H.; Jin, S.; Zhan, W.; Lian, T. Poisson-Distributed Electron-Transfer Dynamics from Single Quantum Dots to C_{60} Molecules. *ACS Nano* **2011**, *5*, 613−621.

DOI: 10.1021/acs.jpclett.5b01256
J. Phys. Chem. Lett. 2015, 6, 2841−2846